

Article

The Effect of Deposition Parameters on the Structure and Mechanical Properties of Chromium Oxide Coatings Deposited by Reactive Magnetron Sputtering

Masoud Mohammadtaheri, Qiaoqin Yang *, Yuanshi Li and Jesus Corona-Gomez

Department of Mechanical Engineering, University of Saskatchewan, 57 Campus Drive, Saskatoon, SK S7H 5A9, Canada; msctaheri@gmail.com (M.M.); yuanshi_li@yahoo.com (Y.L.); jcoronaggis@gmail.com (J.C.-G.)

* Correspondence: qiaoqin.yang@usask.ca; Tel.: +1-306-966-5470

Received: 7 February 2018; Accepted: 13 March 2018; Published: 19 March 2018

Abstract: Appropriate conditions for depositing hard Cr₂O₃ coatings by reactive sputtering techniques have yet to be defined. To fill this gap, the effect of principal deposition parameters, including deposition pressure, temperature, Cr-target voltage, and Ar/O₂ ratio, on both the structure and mechanical properties of chromium oxide coatings was investigated. A relationship between processing, structure, and the mechanical properties of chromium oxide coatings was established. Scanning electron microscopy (SEM), X-ray diffraction (XRD), Raman spectroscopy, and X-ray Photoelectron Spectroscopy (XPS) were used to characterize the morphology, structure, and chemical compositions of the coatings that were prepared. An optical profilometer was employed to measure both the roughness and thickness of the coatings. The hardness and Young's modulus of the coatings both as-deposited and after annealing conditions were measured by nanoindentation. The results showed that depositing hard Cr₂O₃ coatings is a highly critical task, requiring special deposition conditions. Cr₂O₃ coatings with a high hardness of approximately 25 GPa could be achieved at room temperature, at a low pressure of 1.6×10^{-1} Pa, where Cr-target voltage and oxygen content were 260 V and between 15–25 vol % of total gas, respectively. A dense stoichiometric Cr₂O₃ structure was found to be responsible for the high chromium oxide coating hardness observed.

Keywords: chromium oxide; coatings; reactive magnetron sputtering; hardness; structure

1. Introduction

Bulk Cr₂O₃ is one of the hardest oxides, with a hardness of 29.5 GPa [1–4], and can be deposited as a protective coating for many purposes, due to its high wear resistance, low coefficient of friction, and excellent corrosion resistance [5–7]. Many methods, including plasma-spray [8–10], sputtering [11,12], chemical vapor deposition (CVD) [13], and pulsed laser deposition [14], have been used to produce Cr₂O₃ coatings. However, among them, only sputtering techniques have so far been successful in producing Cr₂O₃ coatings with a hardness value close to that of bulk Cr₂O₃ [3,12,15,16]. Nevertheless, chromium oxide coatings deposited by sputtering methods can also show weak mechanical properties if appropriate deposition parameters are not selected during the deposition process. Chromium oxides exist in various forms (phases), including CrO₃, CrO_{2.906}, Cr₈O₂₁, Cr₅O₁₂, CrO₂, Cr₂O₃, Cr₃O₄, CrO, and Cr₃O, due to the different valance states of metallic chromium [1,16,17]. Thus, the various forms of chromium oxides, with different microstructures and chemical compositions, could be the main reason for the wide range of mechanical properties in chromium oxide coatings deposited under nonequilibrium sputtering conditions at low temperatures and pressure. In this context, Hones et al. [3] investigated the effect of deposition temperature and oxygen partial pressure

on the hardness of chromium oxide coatings deposited by a reactive magnetron sputtering technique. They showed that Cr₂O₃ coatings with good adhesion and a hardness value up to 32 GPa can be obtained for 1–2 μm thick films when substrate temperatures exceeded 500 K and oxygen partial pressure is between 15% and 25%. Moreover, Luo et al. [12,15] used the same method to evaluate the effect of oxygen flow rate and radio frequency (RF) powers on the microstructure and hardness of chromium oxide coatings. They illustrated that chromium oxide coatings with high hardness can be obtained at a high oxygen flow rate and a low RF power. We tried to deposit hard Cr₂O₃ coatings using the same deposition parameters reported by these researchers, who successfully obtained hard Cr₂O₃ coatings using the reactive magnetron sputtering technique [3,6,12,15,16], but unfortunately, the hardness of our coatings was as low as 4 GPa. This repeatability problem could be associated with the lack of comprehensive research on the relationships between the processing, structure, and mechanical properties of chromium oxide coatings deposited by reactive magnetron sputtering. Furthermore, the hardness value reported in the majority of the literature seems to have high uncertainty due to the lack of international standards. According to the authors' knowledge, no previous research exists considering all principal deposition parameters together to show the importance of each deposition parameter in achieving chromium oxide coatings with a hardness value close to the bulk counterpart. Therefore, in the current research, reactive RF magnetron sputtering was used to deposit chromium oxide coatings, considering the effects of principal deposition parameters, including deposition pressure, temperature, Cr-target voltage, and Ar/O₂ ratio, and the correlation between structure, phase composition, and hardness of the chromium oxide coatings was established. A microstructural and phase compositional analysis confirmed that the dense stoichiometric Cr₂O₃ structure is responsible for the high hardness of chromium oxide coatings obtained in a specific deposition condition.

2. Materials and Methods

All the chromium oxide coatings were deposited for 10 h on silicon (100) wafers using a RF-magnetron sputtering system (SPLD620-FLR made by Plasmionique Inc., Rimouski, QC, Canada) from a 76.2 mm-diameter Cr target (99.95% pure) in plasma of Ar + O₂. The chamber was evacuated to a vacuum of 2.6×10^{-5} Pa before deposition. The target–substrate distance was kept to 50 mm and the substrates were rotating at a speed of 5 rpm. Depositions were performed at room temperature (without external substrate heating) using a Cr target voltage of 260 V. The Ar/O₂ ratio was 6, while the deposition pressure varied from 1 to 1.6×10^{-1} Pa. In the second series, the deposition temperature altered between room temperature and 400 °C, with deposition pressure constant at 1.6×10^{-1} Pa. In the third series, Cr target voltage was tuned from 180 V to 300 V, while deposition pressure and deposition temperatures were 1.6×10^{-1} Pa and room temperature, respectively. In the final series, the Ar/O₂ ratio changed between 6 and 3, whereas deposition pressure, Cr target voltage, and temperature remained constant at 1.6×10^{-1} Pa, 260 V, and room temperature, respectively. Detailed deposition parameters are summarized in Table 1. This experimental design allows for the investigation of the individual effects of each deposition parameter on the structure and mechanical properties of chromium oxide coatings. The Optical profilometer (New View 8000), manufactured by Zygo Corporation, Middlefield, CT, USA, with a 50X Mirau objective and standard filter type (bandwidth 125 nm and center wavelength 550 nm), was used to measure both the mean roughness (R_a) and thickness of the coatings. The roughness and thickness value of each coating was based on three measurements and an average value was reported. The phase composition of the coatings was investigated by XRD (Rigaku XRD ultima IV) using CuK α radiation at grazing incidence ($\theta = 7^\circ$). The obtained XRD patterns were matched with the Joint Committee on Powder Diffraction Standards (JCPDS) database, using X'Pert HighScore Plus software to identify the chromium oxide peaks. Raman spectroscopy was also performed on the coatings using a Renishaw 2000 spectroscope with an Argon ($\lambda = 514$ nm, $P = 0.5$ mW) laser source to support the XRD patterns and identify the different oxide

states. Calibration was done using a silicon reference sample before the Raman measurements, and the peak positions were determined using Wire.3.3 software.

Table 1. Detailed deposition parameters for the deposition of chromium oxide coatings.

Parameter	Cr Voltage (V)	Ar Flow Rate (sccm)	O ₂ Flow Rate (sccm)	Temperature (°C)	Pressure (Pa)
Pressure Change	260	30	5	25	1
					0.82
					0.29
					0.16
Temperature Change	260	30	5	25	0.16
				150	
				300	
				400	
Cr Voltage Change	300	30	5	25	0.16
	260				
	220				
	180				
Ar/O ₂ Ratio Change	260	30	5	25	0.16
		25			
		20			
		15			

X-ray Photoelectron Spectroscopy (XPS) with Al K α radiation was used to characterize the chemical states of the coatings. Before XPS measurements, the surface of the coatings was sputter-etched with Ar ions for 20 s to remove surface contaminants. Due to the insulating properties of oxide materials, during XPS analysis a charge correction was also accomplished by monitoring a high resolution spectrum of adventitious hydrocarbon on the surface of the samples. Scanning Electron Microscopy (SEM) was employed to observe the surface morphology of the coatings. The mechanical properties of the coatings (hardness and Young's modulus) were measured according to ISO standard 14577-1 [18] using a nanoindentation technique with a three-face pyramid Berkovich indenter. The load-displacement graphs obtained during nanoindentation were interpreted using the Oliver–Pharr method [19], and the hardness values reported were an average value based on five indentations at 3 mN load. During the measurements, the indentation depth was kept 20 times larger than the surface roughness and lower than 10% of the coating thickness, in order to avoid the effect of surface roughness and substrate hardness on the measured hardness values. The thermal stability of the coatings was evaluated by a 3 h annealing procedure in the air of a tube furnace at temperatures in the range 400–700 °C, with a 10 °C/min heating and cooling rate. The hardness of the coatings was measured after the annealing treatments using the nanoindentation method.

3. Results and Discussion

3.1. Roughness and Thickness of Coatings

Figure 1 shows the effects of deposition parameters on the thickness and roughness of chromium oxide coatings. The thickness of the coatings (the deposition rate) was strongly related to the deposition pressure. Coating thickness increased consistently with increasing deposition pressure and reached a maximum at 0.82 Pa (Figure 1a). This trend was expected since the Argon ions (Ar⁺), responsible for sputtering of Cr-target, increased as the deposition pressure increased. At deposition pressures higher than 0.82 Pa, the deposition rate decreased again, which could be attributed to the collisions occurring between the sputtered atoms and gas molecules when the average free path of gas molecules (λ) decreased at higher pressures [20].

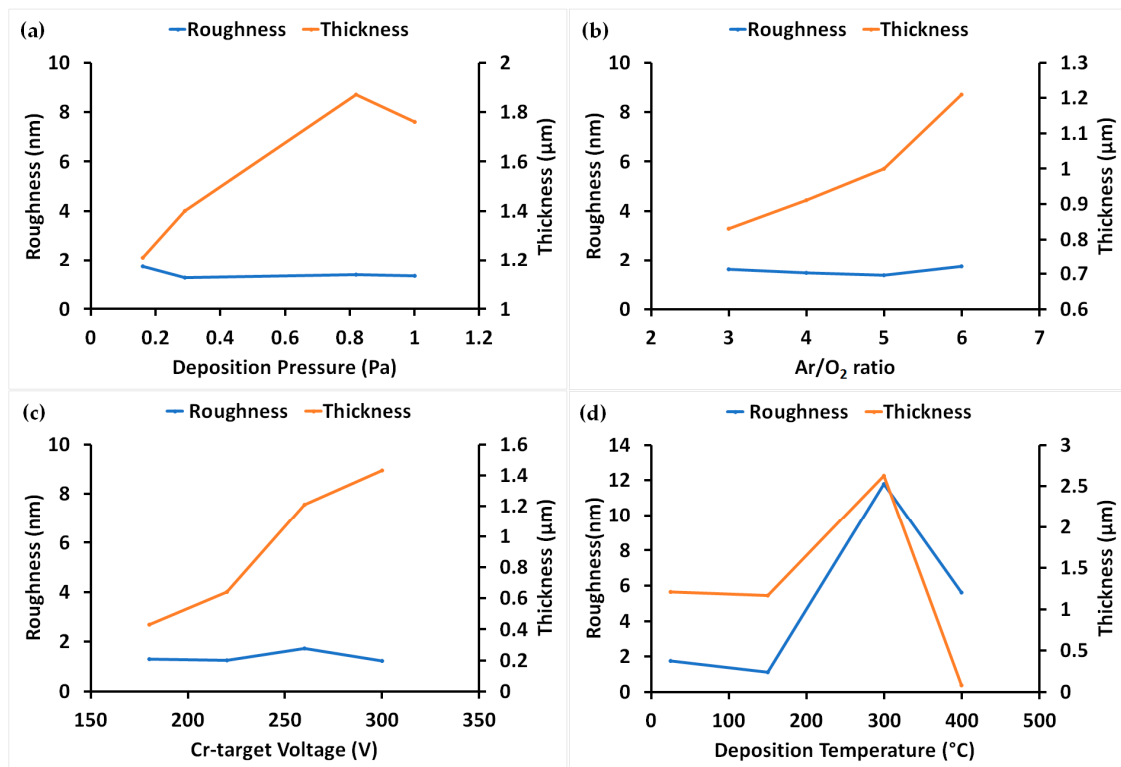


Figure 1. The effect of deposition parameters on the roughness (R_a) and thickness of chromium oxide coatings: (a) Pressure; (b) Ar/O₂ ratio; (c) Cr-target voltage; and (d) Temperature. Standard deviations are too small to be seen in the graphs.

Thickness also increased with the increasing Ar/O₂ ratio and sputtering voltage (Figure 1b,c). Argon ions are responsible for the sputtering of the Cr target, so as the Ar/O₂ ratio increases at a constant oxygen flow rate the sputtering rate rises. The increment in the energy and quantity of plasma ions as the sputtering voltage increases, is responsible for the increase in the deposition rate.

Thickness analysis of the chromium oxide coatings deposited under various deposition temperatures is illustrated in Figure 1d. The thickness of coatings substantially increased at 300 °C. Since the sputtering rate of the Cr-target was not related to the substrate temperature, the increasing coating thickness with the increasing temperature may be correlated with other factors.

Figure 2 shows the SEM cross-section and surface morphology of coatings deposited at room temperature and 300 °C. The coatings deposited at 300 °C showed a spongy structure (Figure 2a) compared to the dense structure of the coatings deposited at room temperature (Figure 2c). A flake-like surface morphology was observed for the coatings deposited at 300 °C (Figure 2b), which can be attributed to the crystallization of coatings at high temperatures; whereas, a nanocrystalline morphology was observed for the coatings deposited at room temperature (Figure 2d). According to structural analysis by SEM (Figure 2a,c), the porous structure of the coatings due to the volatilization of Cr₂O₃ at high temperatures, which prevents the coatings forming a dense and compact structure, is thought to be the reason for the high thickness for coatings deposited at 300 °C. The volatilization of Cr₂O₃ at high temperatures has already been confirmed in ceramics composed of Cr₂O₃, phase sintered at high temperatures, and it has been shown in Cr-O phase diagrams [21,22]. Under-dense chromium oxide coatings were also observed by Pedersen et al. [23] for coatings deposited at 300 °C by reactive inductively coupled plasma magnetron sputtering. They assumed the shadowing effect was responsible for the low density of the coatings deposited at high temperatures, which is not understandable to the present authors. At 400 °C, the coatings completely lost their adhesion and integration so that the coatings were indeed particles which could be easily wiped out by a tissue

paper. The excessive volatilization of Cr_2O_3 at high temperatures and low pressures could also be responsible for the very low thickness (80 nm) of coatings deposited at 400 °C.

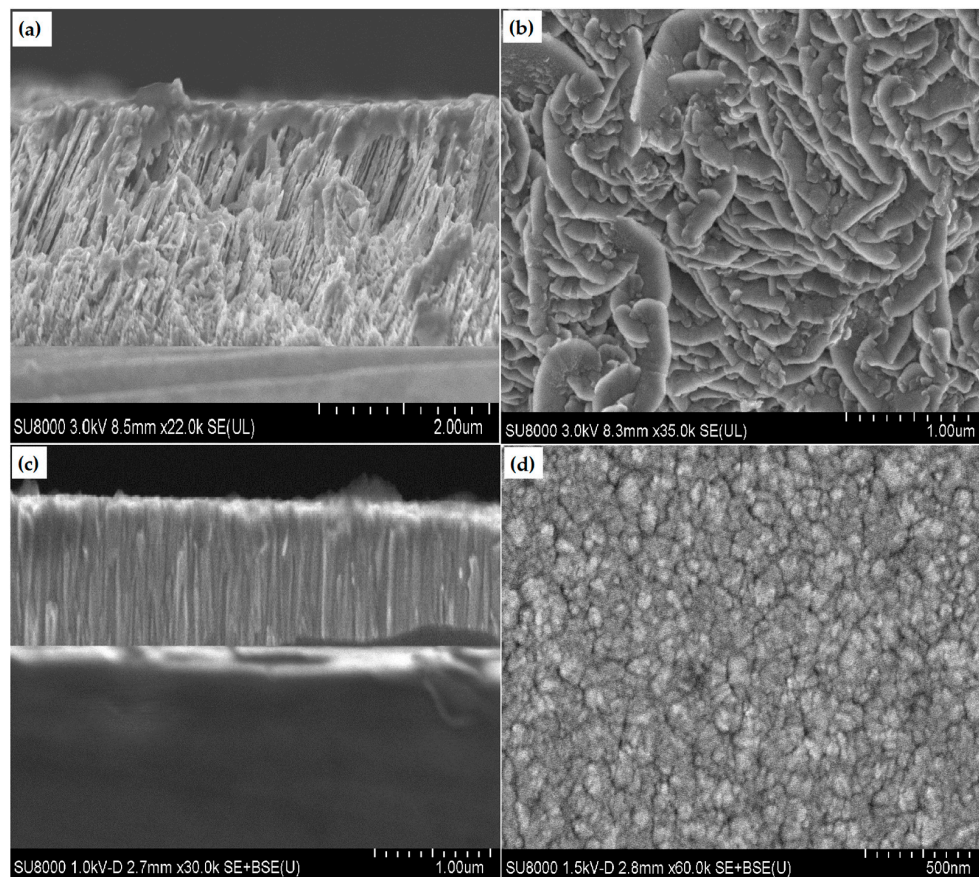


Figure 2. SEM cross-section and surface micrographs of chromium oxide coatings deposited at 300 °C (a,b) and room temperature (c,d), respectively.

Among all the deposition parameters, only substrate temperature had a substantial effect on the surface roughness of the coatings (Figure 1d). All of the coatings deposited at room temperature showed very smooth surfaces, in the range of 1–2 nm, indicating that the coatings had a nanocrystalline or amorphous structure. The SEM results were consistent with the optical profilometer data, showing that a porous structure and well-crystallized morphology are responsible for increasing both the thickness and roughness of coatings deposited 300 °C, respectively.

3.2. Structure and Phase Composition of Coatings

The structural analysis conducted by XRD (not shown here) on chromium oxide coatings deposited at different deposition pressures showed that the coatings had an amorphous structure, regardless of the deposition pressure, as they showed only a broad peak centered at the beginning of the patterns. However, the presence of crystalline phases was not completely excluded, since crystalline phases cannot be detected if their fraction falls below the XRD detection limit or the crystalline size is very small. The amorphous structure of coatings can be attributed to low substrate temperatures. Since Raman spectroscopy is a well-known method for the characterization of both amorphous and crystalline materials [24], this method was employed to complement the XRD results and the results are shown in Figure 3. Raman shifts at 648 cm^{-1} , 607 cm^{-1} , 548 cm^{-1} , 348 cm^{-1} , and 303 cm^{-1} can be assigned to the Raman modes of Cr_2O_3 [25–27]; whereas, the broad peaks

at 691 cm^{-1} and $800\text{--}900\text{ cm}^{-1}$ can be assigned to amorphous CrO_2 and either CrO_3 or Cr_8O_{21} , respectively [14,26,28,29].

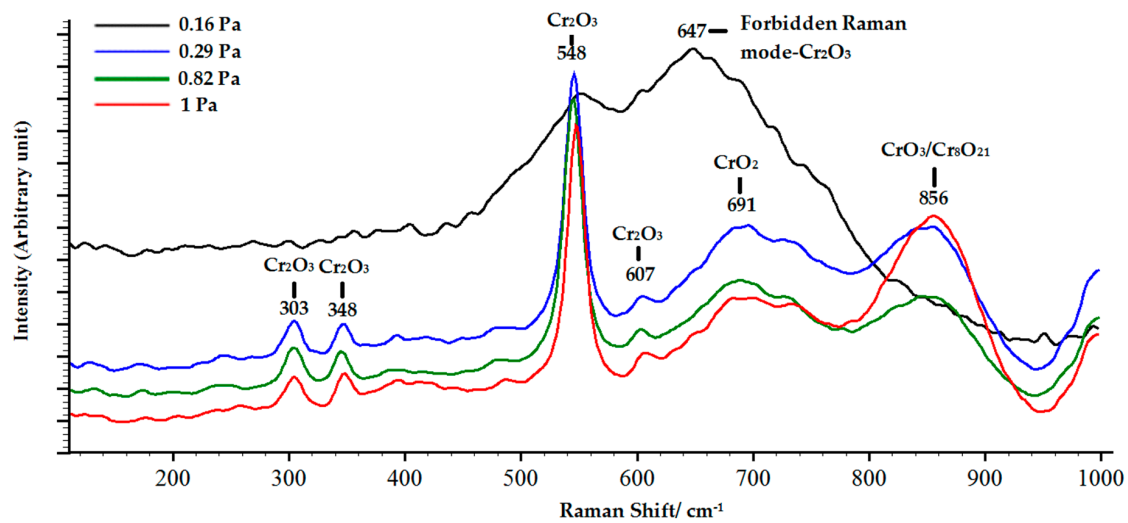


Figure 3. Raman spectra of chromium oxide coatings deposited at different pressures.

With a decrease in deposition pressure from 1 to 0.16 Pa, the Raman peaks related to CrO_2 and $\text{CrO}_3/\text{Cr}_8\text{O}_{21}$ phases disappeared and the intensity of Cr_2O_3 Raman shifts decreased significantly, indicating that the coatings transformed from a multi-phase structure to a single-phase, amorphous Cr_2O_3 structure. Thus, increasing the deposition pressure induced the formation of amorphous chromium oxide phases with a higher oxidation state. This was likely related to the elevated oxygen level in the deposition atmosphere when the deposition pressure increased. The high-resolution Cr 2p XPS analysis performed on the chromium oxide deposited at 0.16 Pa (Figure 4) confirmed that Cr_2O_3 was the only phase that existed in the coatings. According to the XPS data, the Cr $2p_{3/2}$ spectrum binding energy was 576.6, and the difference between the Cr $2p_{3/2}$ and Cr $2p_{1/2}$ binding energies was 9.7, which corresponded to Cr_2O_3 [30]. Therefore, the Raman peak observed at 647 cm^{-1} for the chromium oxide deposited at 0.16 Pa can be attributed to the forbidden Raman modes of Cr_2O_3 activated in amorphous materials [17,31].

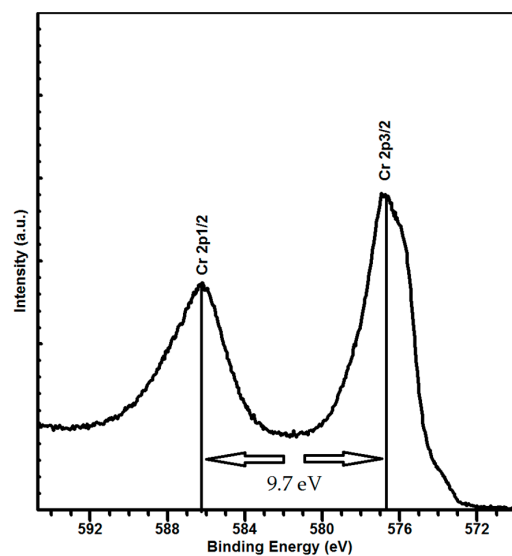


Figure 4. The high-resolution Cr 2p XPS spectrum of coatings deposited at 0.16 Pa pressure.

The XRD patterns of the coatings, deposited at different temperatures, are shown in Figure 5a. All the crystalline peaks belonged to the hexagonal Cr_2O_3 structure, according to (PDF-98-009-7850) databases. The XRD results showed that the crystallization developed throughout the coatings at a temperature of 150 °C. More crystalline Cr_2O_3 peaks could be observed for the coatings deposited at 300 °C. The Raman spectra of the coatings deposited at a temperature higher than room temperature showed single-phase crystalline Cr_2O_3 peaks (Figure 5b). The Raman results were in agreement with the XRD data and were also consistent with the thermodynamic data, since they previously showed that all types of chromium oxide phases transformed to a stable Cr_2O_3 phase with increasing temperature [21,32,33].

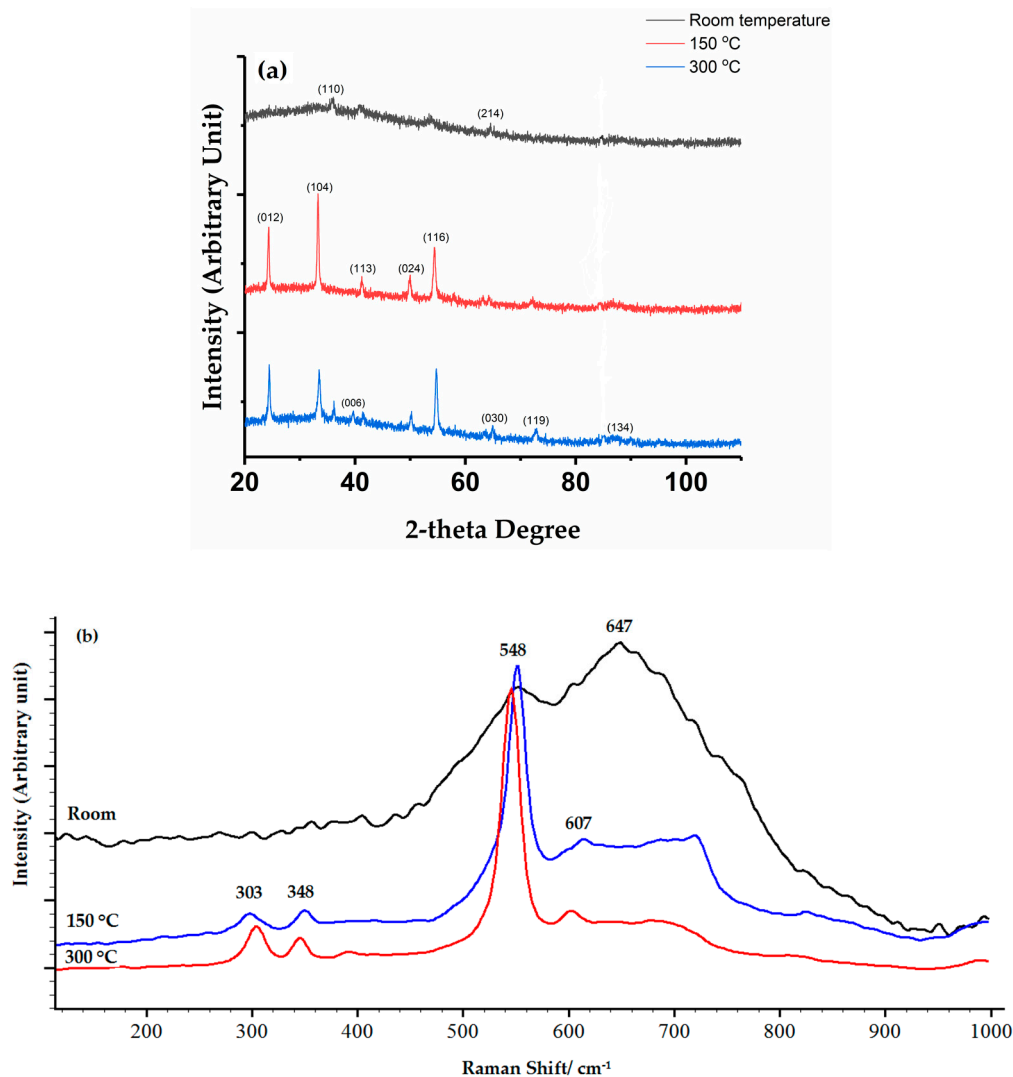


Figure 5. (a) XRD patterns and (b) Raman spectra of chromium oxide coatings deposited at different temperatures.

The chromium oxide coatings also showed a major amorphous structure, regardless of the Cr-target voltage, as long as they were deposited at room temperature (Figure 6a). According to the Raman spectra of the coatings deposited at 180 and 220 V (Figure 6b), they were mostly composed of the amorphous CrO_3 phase, as broad Raman peaks can be seen at 800–900 cm^{-1} . They also showed main Cr_2O_3 Raman shifts at 548 cm^{-1} . The amount of the Cr_2O_3 phase is believed to be negligible, according to the low intensity of the Cr_2O_3 peak. The Si substrate Raman peak at 520 cm^{-1} was also observed in the Raman spectrum of coatings deposited at 180 V due to the very low thickness of the

coatings. Nevertheless, the coatings deposited at 260 and 300 V showed only an amorphous Cr_2O_3 peak in both Raman (548 cm^{-1}) and XRD analysis.

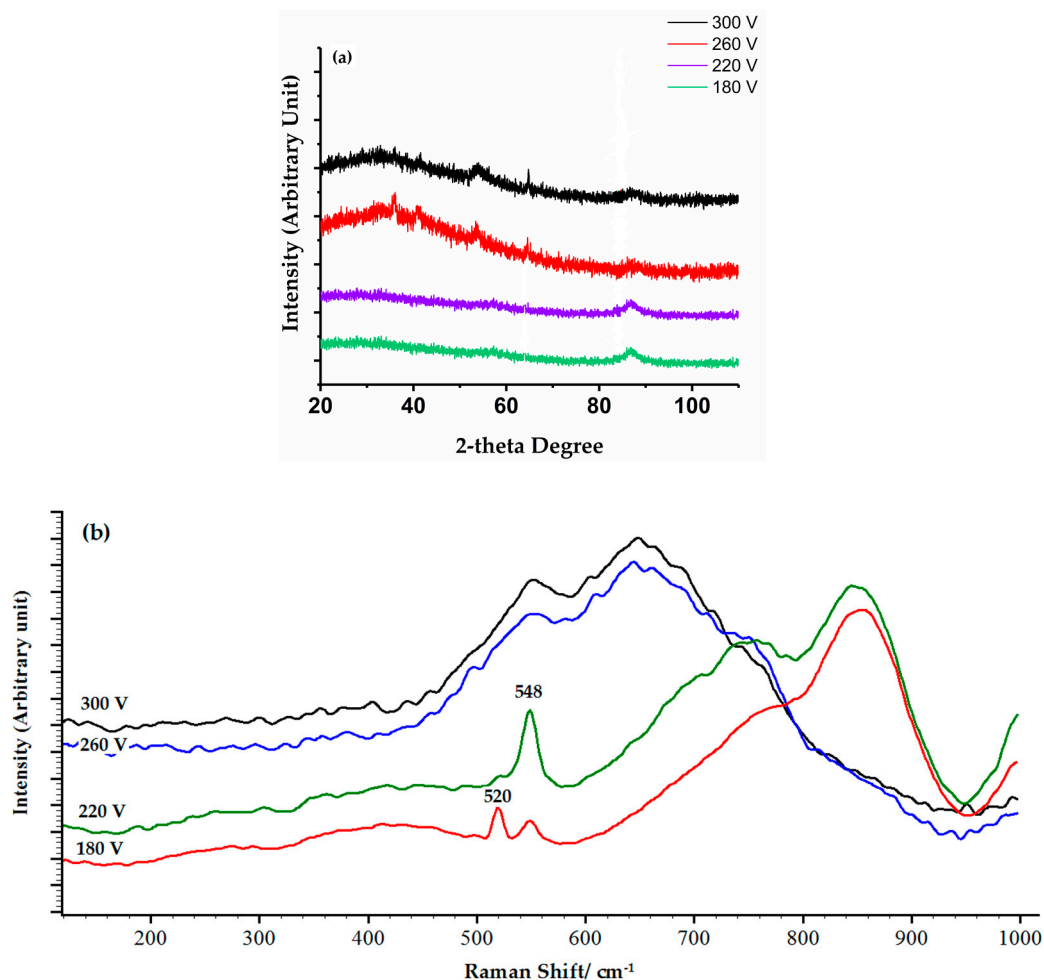


Figure 6. (a) XRD patterns and (b) Raman spectra of chromium oxide coatings deposited at different voltages.

Figure 7 illustrates the high-resolution Cr2p XPS spectra of coatings deposited at 300 V. This revealed the existence of metallic Cr in the coatings. According to XPS data, the Cr $2p_{3/2}$ spectrum could be curve fitted with two separate peak components at binding energies of 574.1 and 576.6, and the difference between the Cr $2p_{3/2}$ and Cr $2p_{1/2}$ binding energies was 9.3 and 9.7, corresponding to metallic Cr and Cr_2O_3 , respectively [30]. From the XPS results, it can be inferred that a small fraction of metallic chromium existed in the structure of the coatings deposited at 300 V, which cannot be detected by XRD and Raman spectroscopy. A deficiency in the oxygen needed to oxidize the excessive amount of sputtered metallic chromium at higher voltages is believed to be the reason why metallic chromium was observed in the coatings.

Contrary to other deposition parameters, changing the Ar/ O_2 ratio from 6 to 3 did not have a considerable effect on both the phase composition and crystal structure of coatings, according to the XRD and Raman spectroscopy results illustrated in Figure 8. All of the coatings showed a mainly amorphous structure and the small diffraction lines detected at $2\theta = 35.95^\circ$, 40.92° , 53.69° , 64.53° and 87.20° belonged to the nano- Cr_2O_3 structure. The broad Raman shift observed at 548 cm^{-1} was assigned to the strongest Raman mode of Cr_2O_3 , which supports the XRD results.

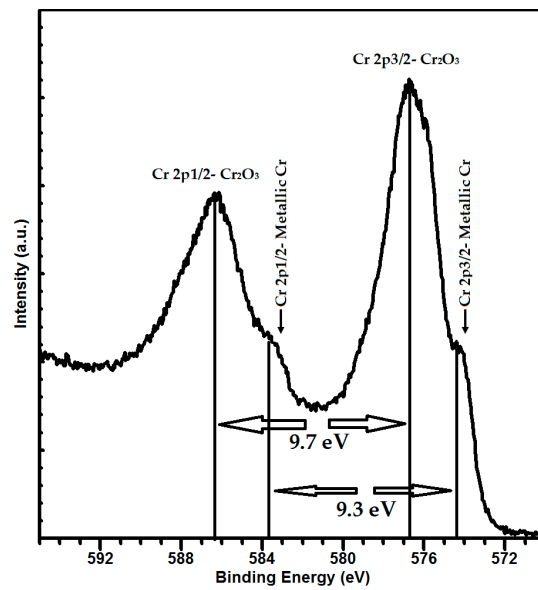


Figure 7. The high-resolution Cr 2p XPS spectrum of coatings deposited at 300 Cr-target voltages.

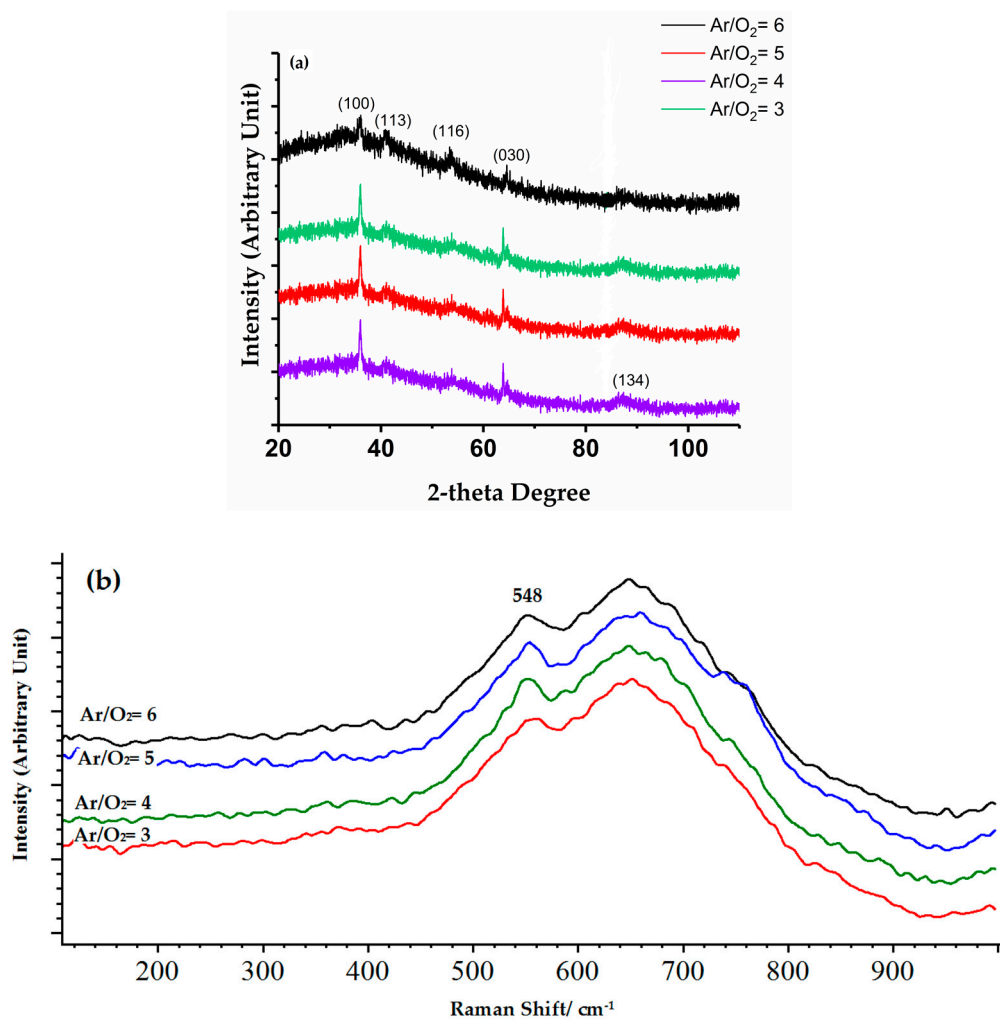


Figure 8. (a) XRD patterns and (b) Raman spectra of chromium oxide coatings deposited at different Ar/O₂ ratios.

3.3. Mechanical Properties of Coatings

In Figure 9a, variation in hardness and Young's modulus as a function of deposition pressure, is displayed. When the deposition pressure was in the range of 1–0.29 Pa, the chromium oxide coatings had an average hardness and Young's modulus value of about 5 and 80 GPa, respectively. This result is consistent with Figure 6 in Kao's [4] research, in which chromium oxide coatings showed a low hardness value of 8 GPa when deposited at a process pressure between 0.5–2.5 Pa. Decreasing the operation pressure to 0.16 Pa, the hardness and Young's modulus of the coatings increased significantly and reached an average hardness and Young's modulus value of about 25 and 289 GPa, respectively, which is near the bulk Cr_2O_3 values reported in previous literature [1–4,34].

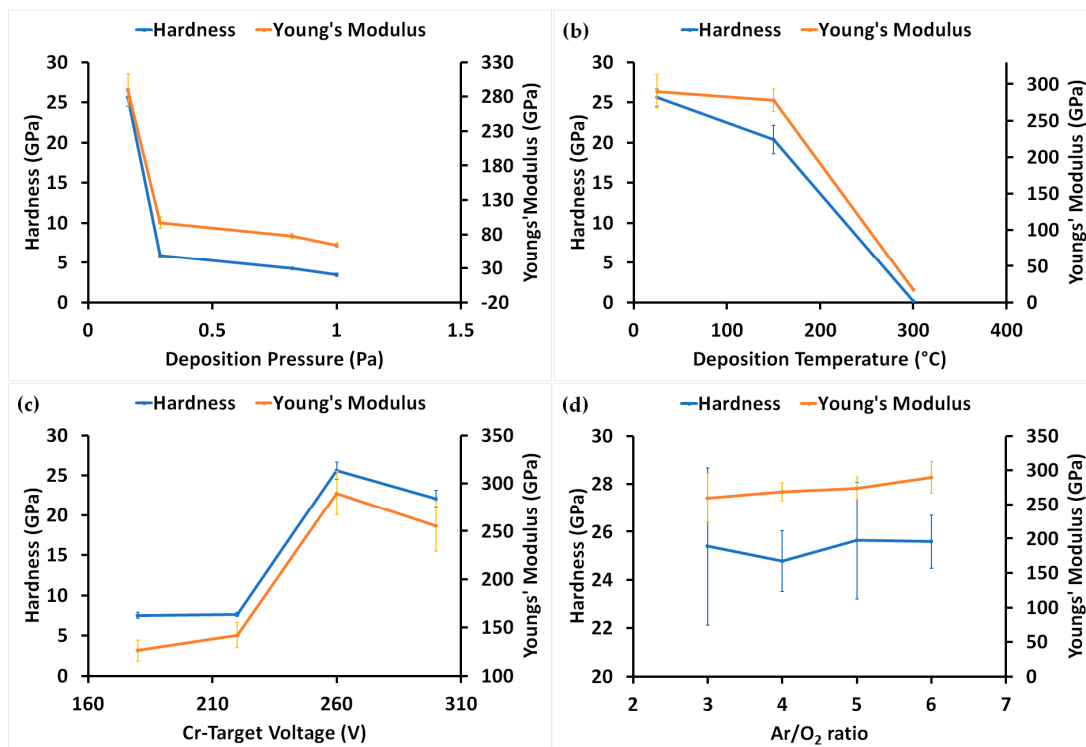


Figure 9. Effect of (a) deposition pressure, (b) deposition temperature, (c) Cr-target voltage, and (d) Ar/O₂ ratio on the hardness and Young's modulus of the coatings. Some of Standard deviations are too small to be seen in the graphs.

According to structural analysis results, it can be inferred that the low hardness of the chromium oxide coatings deposited at higher pressures was due to the formation of mixed chromium oxide phases. It is noteworthy that the coatings that showed mechanical properties near the bulk Cr_2O_3 values at 0.16 Pa consisted of a dense single Cr_2O_3 phase with a nanocrystalline and amorphous structure.

With respect to the substrate temperature, the hardness of the coatings decreased significantly as the deposition temperature increased (Figure 9b). The coatings showed a minimum hardness and Young's modulus of 0.16 and 17 GPa, respectively, when the deposition was performed at 300 °C. Structural analysis showed that the coatings prepared at 300 °C had a porous structure, thus a low density, which is thought to be the main reason for the very low mechanical properties. The coatings deposited at 150 °C had a single-phase crystalline Cr_2O_3 structure with a hardness of 20 GPa, which shows that the hardness of crystalline Cr_2O_3 coatings can also reach the bulk Cr_2O_3 hardness if they are prepared with a dense structure.

There was significant variation in the hardness and Young's modulus of coatings as a function of Cr-target voltage (Figure 9c). A low hardness and Young's modulus of about 7 and 130 GPa,

respectively, was measured for the coatings deposited at low voltages (180 and 220 V). Notably, these coatings were composed of various chromium oxide phases in their structure. The reason for dropping the hardness of the coatings deposited at 300 V is related to the presence of metallic Cr in the structure of the coatings, as the increasing voltage enhanced the amount of metallic chromium sputtered in the chamber so there was not enough oxygen to oxidize all the metallic chromium during the deposition.

Figure 9d shows the influence of the Ar/O₂ ratio on the hardness and Young's modulus of the chromium oxide coatings. The mechanical properties of the coatings remained almost constant, regardless of the Ar/O₂ ratio. This can be attributed to the similar structure and phase composition of coatings obtained under various Ar/O₂ ratios.

3.4. Thermal Stability of Chromium Oxide Coatings

Many applications need coatings which can preserve their mechanical properties at high temperatures. Therefore, the thermal stability and mechanical properties of Cr₂O₃ coatings were investigated while keeping them at elevated temperatures. For this purpose, Cr₂O₃ coatings with an average hardness of 25 GPa were selected for the thermal stability studies performed in the air. The coatings had been deposited at room temperature with a Cr-target voltage of 260 V, deposition pressure of 0.16 Pa, and Ar/O₂ ratio of 6. No delamination was observed for the coatings after heat treatment up to 700 °C, indicating that coatings had good adhesion on Si substrates. Figure 10 shows the hardness variation of Cr₂O₃ coatings with annealing temperatures. The hardness of coatings continuously dropped with an increase in annealing temperature and reached 16 GPa at 700 °C. Several factors were responsible for the hardness reductions, namely transferring from an amorphous to a crystalline structure, stress relaxation, and increasing crystallite size. It is a well-known phenomenon that the crystallite size of materials increases with an increase in annealing temperature due to the diffusion and mobility of grain boundaries at elevated temperatures. The structural changes and increase in crystalline size with annealing temperature in chromium oxide coatings was confirmed by the Raman data (Figure 11). According to the Raman results, the amorphous structure of the coatings did not change at 300 °C, but transferred to a well crystallized one at 700 °C. Moreover, different research [3,4] has shown that chromium oxide coatings deposited by PVD techniques possess high compressive stress. This stress can add to the hardness of coatings, which is relieved with the annealing procedure, thus decreasing the hardness of coatings.

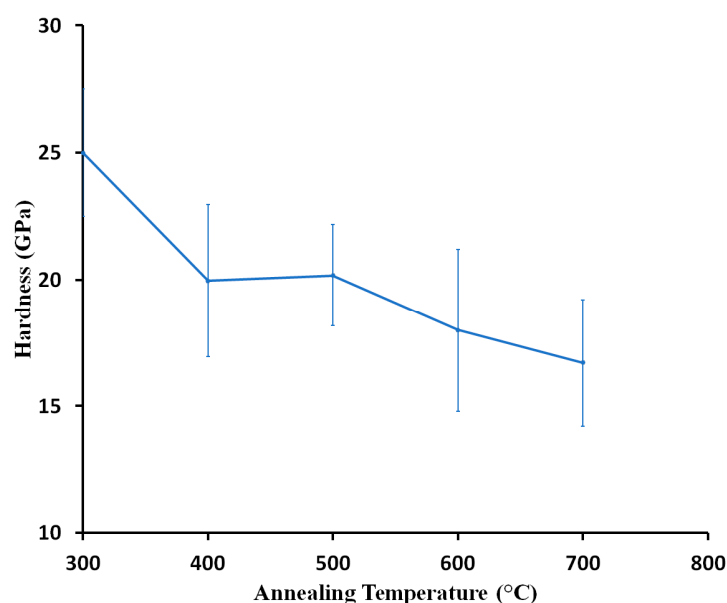


Figure 10. The effect of annealing temperature on the average hardness of Cr₂O₃ coatings.

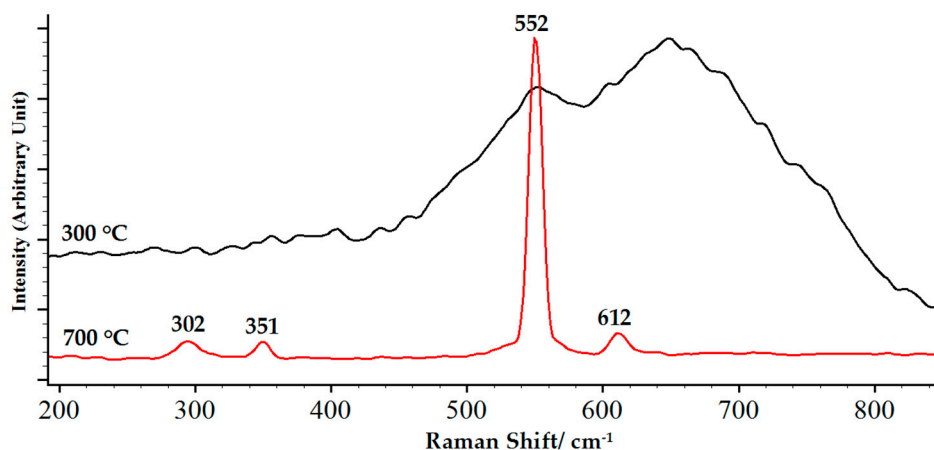


Figure 11. The effect of annealing temperatures on the crystal structure of hard chromium oxide coatings.

4. Conclusions

A thorough investigation was conducted to explore the appropriate conditions for depositing hard chromium oxide coatings using a reactive magnetron sputtering technique. A correlation between deposition parameters and the microstructure, phase composition, and mechanical properties of chromium oxide coatings was established. The results showed that Cr_2O_3 coatings with a high hardness of approximately 25 GPa could be achieved at room temperature, at a low pressure of 1.6×10^{-1} Pa, where Cr-target voltage and oxygen content were 260 V and between 15–20 vol % of total gas, respectively. A dense stoichiometric Cr_2O_3 structure was responsible for the high hardness observed. The structure and mechanical properties of the coatings did not show any sensitivity to the amount of oxygen when it changed between 15–25 vol % of total gas. However, other deposition parameters, namely temperature, pressure, and Cr-target voltage had a huge impact on the final structure, and thus, the mechanical properties of the coatings. The hard Cr_2O_3 coatings exhibited poor thermal stability at high temperatures and their hardness dropped to 16 GPa after annealing at 700 °C.

Acknowledgments: This work was supported by the Natural Sciences and Engineering Research Council of Canada (NSERC), the Canada Foundation for Innovation (CFI), Western Economic Diversification Canada, and the University of Saskatchewan. The authors would like to thank George Belev for performing XPS and Jianfeng Zhu for the grazing incidence XRD measurements.

Author Contributions: Masoud Mohammadtaheri conceived and designed the experiments, performed the experiments, and wrote the paper. Qiaoqin Yang and Yuanshi Li helped in analyzing the data and revising the manuscript. Jesus Corona-Gomez contributed reagents/materials/analysis tools.

Conflicts of Interest: The authors declare no conflict of interest. The founding sponsors had no role in the design of the study; in the collection, analyses, or interpretation of data; in the writing of the manuscript, and in the decision to publish the results.

References

1. Kainarskii, I.S.; Degtyareva, E.V. Chromic oxide as refractory material. *Refractories* **1977**, *18*, 42–47. [[CrossRef](#)]
2. Samsonov, G.V. *The Oxide Handbook*; Springer: Boston, MA, USA, 1973.
3. Hones, P.; Diserens, M.; Lévy, F. Characterization of sputter-deposited chromium oxide thin films. *Surf. Coat. Technol.* **1999**, *120–121*, 277–283. [[CrossRef](#)]
4. Kao, A.S.; Doerner, M.F.; Novotny, V.J. Processing effects on the tribological characteristics of reactively sputtered chromium oxide (Cr_2O_3) overcoat films. *J. Appl. Phys.* **1989**, *66*, 5315–5321. [[CrossRef](#)]
5. Ji, A.L.; Wang, W.; Song, G.H.; Wang, Q.M.; Sun, C.; Wen, L.S. Microstructures and mechanical properties of chromium oxide films by arc ion plating. *Mater. Lett.* **2004**, *58*, 1993–1998. [[CrossRef](#)]
6. Bhushan, B.; Theunissen, G.S.A.M.; Li, X.D. Tribological studies of chromium oxide films for magnetic recording applications. *Thin Solid Films* **1997**, *311*, 67–80. [[CrossRef](#)]

7. Pang, X.; Gao, K.; Luo, F.; Yang, H.; Qiao, L.; Wang, Y.; Volinsky, A.A. Annealing effects on microstructure and mechanical properties of chromium oxide coatings. *Thin Solid Films* **2008**, *516*, 4685–4689. [[CrossRef](#)]
8. Dong, S.; Song, B.; Hansz, B.; Liao, H.; Coddet, C. Microstructure and properties of Cr₂O₃ coating deposited by plasma spraying and dry-ice blasting. *Surf. Coat. Technol.* **2013**, *225*, 58–65. [[CrossRef](#)]
9. Singh, V.P.; Sil, A.; Jayaganthan, R. Wear of plasma sprayed conventional and nanostructured Al₂O₃ and Cr₂O₃, based coatings. *Trans. Indian Inst. Met.* **2012**, *65*, 1–12. [[CrossRef](#)]
10. Babu, P.S.; Sen, D.; Jyothirmayi, A.; Krishna, L.R.; Rao, D.S. Influence of microstructure on the wear and corrosion behavior of detonation sprayed Cr₂O₃-Al₂O₃ and plasma sprayed Cr₂O₃ coatings. *Ceram. Int.* **2018**, *44*, 2351–2357. [[CrossRef](#)]
11. Contoux, G.; Cosset, F.; Célérier, A.; Machet, J. Deposition process study of chromium oxide thin films obtained by d.c. magnetron sputtering. *Thin Solid Films* **1997**, *292*, 75–84. [[CrossRef](#)]
12. Luo, F.; Gao, K.; Pang, X.; Yang, H.; Qiao, L.; Wang, Y. Characterization of the mechanical properties and failure modes of hard coatings deposited by RF magnetron sputtering. *Surf. Coat. Technol.* **2008**, *202*, 3354–3359. [[CrossRef](#)]
13. Carta, G.; Natali, M.; Rossetto, G.; Zanella, P.; Salmaso, G.; Restello, S.; Rigato, V.; Kaciulis, S.; Mezzi, A. A comparative study of Cr₂O₃ thin films obtained by MOCVD using three different precursors. *Chem. Vap. Depos.* **2005**, *11*, 375–380. [[CrossRef](#)]
14. Monnereau, O.; Tortet, L.; Grigorescu, C.E.A.; Savastru, D.; Iordanescu, C.R.; Guinneton, F.; Notonier, R.; Tonetto, A.; Zhang, T.; Mihailescu, I.N.; et al. Chromium oxides mixtures in PLD films investigated by Raman spectroscopy. *J. Optoelectron. Adv. Mater.* **2010**, *12*, 1752–1757.
15. Luo, F.; Pang, X.; Gao, K.; Yang, H.; Wang, Y. Role of deposition parameters on microstructure and mechanical properties of chromium oxide coatings. *Surf. Coat. Technol.* **2007**, *202*, 58–62. [[CrossRef](#)]
16. Lin, J.; Sproul, W.D. Structure and properties of Cr₂O₃ coatings deposited using DCMS, PDCMS, and DOMS. *Surf. Coat. Technol.* **2015**, *276*, 70–76. [[CrossRef](#)]
17. Barshilia, H.C.; Rajam, K.S. Growth and characterization of chromium oxide coatings prepared by pulsed-direct current reactive unbalanced magnetron sputtering. *Appl. Surf. Sci.* **2008**, *255*, 2925–2931. [[CrossRef](#)]
18. *ISO 14577-1 Instrumented Indentation Test for Hardness and Materials Parameters*; ISO: Geneva, Switzerland, 2015.
19. Oliver, W.C.; Pharr, G.M. An improved technique for determining hardness and elastic modulus using load and displacement sensing indentation experiments. *Mater. Res. Soc.* **1992**, *7*, 1564–1583. [[CrossRef](#)]
20. Wu, S.; Chen, H.; Du, X.; Liu, Z. Effect of deposition power and pressure on rate deposition and resistivity of titanium thin films grown by DC magnetron sputtering. *Spectrosc. Lett.* **2016**, *49*, 514–519. [[CrossRef](#)]
21. Fukunaga, O.; Saito, S. Phase Equilibrium in the System CrO₂-Cr₂O₃. *J. Am. Ceram. Soc.* **1968**, *51*, 362–363. [[CrossRef](#)]
22. Ding, Z.; Oberacher, R.; Thummler, F. Cr₂O₃ particulated Reinforced YTZ ceramics with high fracture toughness and strength. In *Science and Technology of Zirconia V*; Badwal, S.P.S., Bannister, M.J., Hannink, R.H.J., Eds.; Technomic Publishing Co.: Lancaster, PA, USA, 1993; pp. 421–431, ISBN 1-56676-073-9.
23. Pedersen, K.; Bøttiger, J.; Sridharan, M.; Sillassen, M.; Eklund, P. Texture and microstructure of Cr₂O₃ and (Cr,Al)₂O₃ thin films deposited by reactive inductively coupled plasma magnetron sputtering. *Thin Solid Films* **2010**, *518*, 4294–4298. [[CrossRef](#)]
24. Kaufmann, E.N. *Characterization of Materials*; John Wiley & Sons, Inc.: Hoboken, NJ, USA, 2003; pp. 698–700, ISBN 0-471-26882-8.
25. Shim, S.-H.; Duffy, T.S.; Jeanloz, R.; Yoo, C.-S.; Iota, V. Raman spectroscopy and X-ray diffraction of phase transitions in Cr₂O₃ to 61 GPa. *Phys. Rev. B* **2004**, *69*, 144107. [[CrossRef](#)]
26. Kikuchi, S.; Kawachi, K.; Kurosawa, M.; Honjho, H.; Yagishita, T. Non-destructive Rapid Analysis Discriminating between Chromium (VI) and Chromium (III) Oxides in Electrical and Electronic Equipment Using Raman Spectroscopy. *Anal. Sci.* **2005**, *21*, 197–198. [[CrossRef](#)] [[PubMed](#)]
27. Brown, D.A.; Cunningham, D.; Glass, W.K. The infrared and Raman spectra of chromium (III) oxide. *Spectrochim. Acta Part A Mol. Spectrosc.* **1968**, *24*, 965–968. [[CrossRef](#)]
28. Iliev, M.; Litvinchuk, A.; Lee, H.-G.; Chu, C.; Barry, A.; Coey, J. Raman spectroscopy of ferromagnetic CrO₂. *Phys. Rev. B* **1999**, *60*, 33–36. [[CrossRef](#)]

29. Stanoi, D.; Socol, G.; Grigorescu, C.; Guinneton, F.; Monnereau, O.; Tortet, L.; Zhang, T.; Mihailescu, I.N. Chromium oxides thin films prepared and coated in situ with gold by pulsed laser deposition. *Mater. Sci. Eng. B Solid-State Mater. Adv. Technol.* **2005**, *118*, 74–78. [[CrossRef](#)]
30. Moulder, J.F.; Stickle, W.F.; Sobol, P.E.; Bomben, K.D. *Handbook of X-ray Photoelectron Spectroscopy*; Perkin-Elmer Corporation: Billerica, MA, USA, 1992; p. 261. [[CrossRef](#)]
31. Berg, R.S.; Yu, P.Y.; Weber, E.R. Raman spectroscopy of intrinsic defects in electron and neutron irradiated GaAs. *Appl. Phys. Lett.* **1985**, *47*, 515–517. [[CrossRef](#)]
32. Yasumasa, G.; Toshio, K. On the Phase Diagram of the Cr-O System at High Pressure of Oxygen and some properties of the Compound CrO_{2+x} . *J. Jpn. Soc. Powder Powder Metallurgy* **1962**, *9*, 109–113. [[CrossRef](#)]
33. Levin, E.M.; Robbins, C.R.; McMurdie, H.F. *Phase Diagrams for Ceramists*; The American Ceramic Society: Westerville, OH, USA, 1964.
34. Saeki, I.; Ohno, T.; Seto, D.; Sakai, O.; Sugiyama, Y.; Sato, T.; Yamauchi, A.; Kurokawa, K.; Takeda, M.; Onishi, T. Measurement of Young's modulus of oxides at high temperature related to the oxidation study. *Mater. High Temp.* **2011**, *28*, 264–268. [[CrossRef](#)]



© 2018 by the authors. Licensee MDPI, Basel, Switzerland. This article is an open access article distributed under the terms and conditions of the Creative Commons Attribution (CC BY) license (<http://creativecommons.org/licenses/by/4.0/>).